

## Protein/Solvent Medium Effects on $Mg^{2+}$ –Carboxylate Interactions in Metalloenzymes

C. Satheesan Babu<sup>†</sup> and Carmay Lim<sup>\*†‡</sup>

*Institute of Biomedical Sciences, Academia Sinica, Taipei 11529, Taiwan, R.O.C., and Department of Chemistry, National Tsing Hua University, Hsinchu 300, Taiwan, R.O.C.*

Received February 21, 2010; E-mail: carmay@gate.sinica.edu.tw

A molecular-level understanding of the role of the protein three-dimensional (3D) structure and its aqueous environment (i.e., the protein matrix) in ligand recognition is critical in modeling protein–ligand interactions. The binding of an essential cofactor to enzymes (e.g., hydrated  $Mg^{2+}$  to nucleases) exemplifies such recognition due to long-range electrostatic forces and a strong dehydration penalty.<sup>1</sup>  $Mg^{2+}$  can bind to an enzyme in different modes, defined by the number of water molecules exchanged for protein ligands. However, the different metal-binding modes may *not* be functionally equivalent (see below). This raises the intriguing question of how an enzyme selects a particular metal-binding mode for catalytic function. The enzyme chosen for study was ribonuclease H (RNase H), which degrades the RNA strand of DNA–RNA hybrids.<sup>2</sup> Here we show that the enzyme can trap a water-rich  $Mg^{2+}$ -binding mode by raising the free-energy barrier to a water-depleted mode. Such a high barrier is shown to emerge from the protein matrix. These results provide new insights into the roles of the protein 3D architecture and the coupled protein–solvent interactions in recognizing a certain ligand-binding mode; these insights may impact structure-based drug design approaches.

A highly conserved DED motif is involved in metal binding in the RNase H family. The first D emerges from a  $\beta$ -sheet, and the E comes from an  $\alpha$ -helix; the second D resides in a fork between the  $\alpha$ -helix and the  $\beta$ -sheet.<sup>3,4</sup> All three carboxylates are highly conserved and catalytically important, but the distance/orientation of the motif's third carboxylate (D) relative to  $Mg^{2+}$  varies in the metal-bound RNase structures: In the  $Mg^{2+}$ -bound X-ray structure of *Escherichia coli* (*E. coli*) RNase HI (PDB entry 1rdd; Figure 1A),<sup>5</sup> two carboxylates (D10, E48) are monodentately bound to  $Mg^{2+}$ , but the third carboxylate (D70) is in the metal's outer shell,  $>4 \text{ \AA}$  from  $Mg^{2+}$ . In the NMR structure of the human immunodeficiency virus type 1 (HIV-1) reverse transcriptase RNase H domain (PDB entry 1o1w; Figure 1A),<sup>6</sup> the  $Mg^{2+}$  position is uncertain even though the structure was solved with 80 mM  $MgCl_2$ . However, the carboxylate orientations suggest that all three carboxylates (D21, E56, D76) are monodentately bound to  $Mg^{2+}$ . In the  $Mg^{2+}$ -bound X-ray structure of maloney murine leukemia virus (MMLV) RNase H (PDB entry 2hb5; Figure 1A),<sup>4</sup> two carboxylates (D28, E66) are monodentately bound to  $Mg^{2+}$ , but the third carboxylate (D87) could be bound in an equilibrium between monodentate and bidentate forms, as a monodentate-bound carboxylate has a free O that is more than  $3.5 \text{ \AA}$  from  $Mg^{2+}$ .

The above structures indicate binding of a single  $Mg^{2+}$  to prokaryotic RNase H (consistent with solution thermodynamic measurements<sup>8</sup>) in three modes. In aqueous solution,  $Mg^{2+}$  is octahedrally hydrated.<sup>9</sup> It is attracted to the enzyme's metal-binding site, which is lined by the three carboxylates from the DED motif,

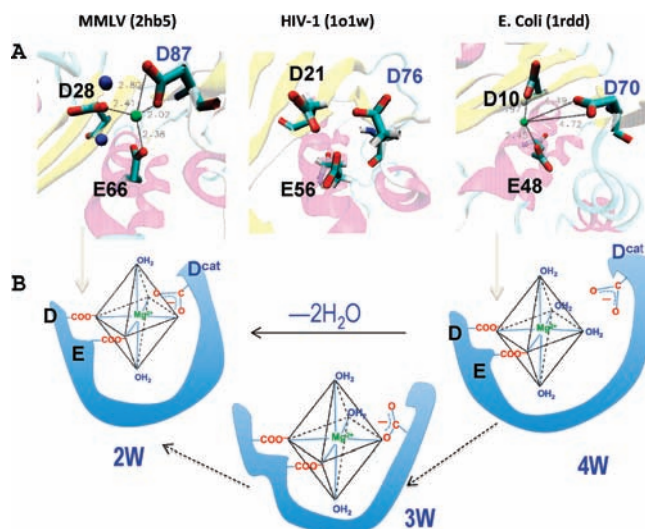


**Figure 1.** (A)  $Mg^{2+}$ -binding sites in RNase H derived from *E. coli* (1rdd), HIV-1 (1o1w), and MMLV (2hb5). The two blue spheres in the 2hb5 structure are metal-bound water O atoms. The D<sup>cat</sup> in the DED motif is labeled in blue. The figures were generated using VMD.<sup>7</sup> (B) Schematic diagram showing the binding of  $Mg[(H_2O)_6]^{2+}$  to the DED<sup>cat</sup> motif of RNase H in different modes.

and binds monodentately to two of the carboxylates with the release of two water molecules (**4W** in Figure 1B). It can also bind to the third carboxylate monodentately (**3W** in Figure 1B) or bidentately (**2W** in Figure 1B) by losing one or two more water molecules, respectively.

The three  $Mg^{2+}$ -binding modes in Figure 1 are *not* functionally equivalent. In *E. coli* RNase HI, mutation of the outer-shell Asp (D70) to Asn inactivates the enzyme even in the presence of  $Mg^{2+}$ , indicating that D70 is catalytically essential.<sup>5</sup> Notably, when the catalytically essential D<sup>cat</sup> carboxylate of the DED<sup>cat</sup> motif is bidentately bound to  $Mg^{2+}$ , it cannot serve as a proton or H-bond acceptor during catalysis. Furthermore, the electrostatic interactions of the nucleophile and/or substrate with an *anionic* complex having three  $Mg^{2+}$ -bound carboxylates would differ from those with the *neutral* complex having two  $Mg^{2+}$ -bound carboxylates.

Since quantum-mechanical and free-energy-perturbation calculations in protein solution show that the different  $Mg^{2+}$ -binding modes in Figure 1B are nearly equally stable (with **2W** more stable than **4W** by  $\sim 2 \text{ kcal/mol}$ ),<sup>10</sup> how can the protein differentiate between a functional metal-binding mode and other modes that are also energetically favorable? We postulated that there might be a significant free-energy barrier for binding of an outer-shell carboxylate to  $Mg^{2+}$ . Hence, the free-energy barriers for going from the **4W** mode to the **2W** mode with **3W** as intermediate in *E. coli*, HIV-1, and MMLV RNase H were computed from molecular dynamics simulations in explicit water with and without umbrella

<sup>†</sup> Academia Sinica.

<sup>‡</sup> National Tsing Hua University.

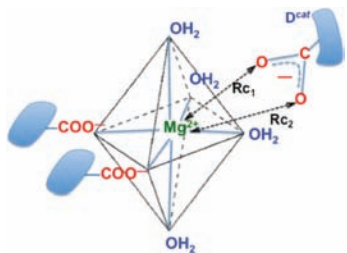


Figure 2. The reaction coordinate ( $R_c$ ) is defined as  $(R_{c1} + R_{c2})/2$ .

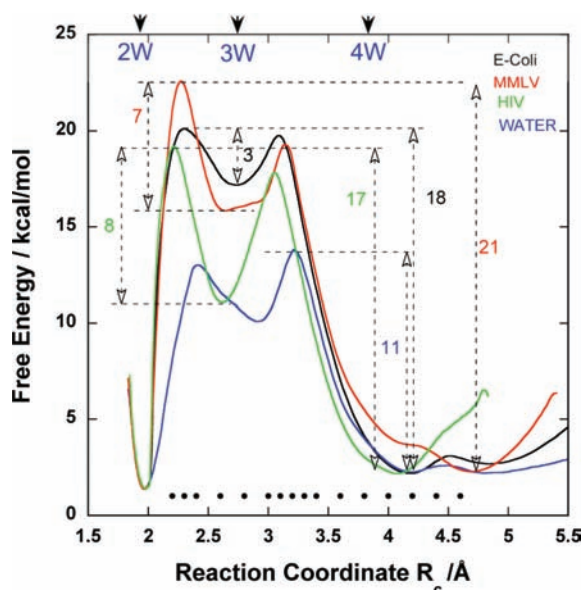


Figure 3. Free energy as a function of the reaction coordinate in *E. coli* (black), HIV-1 (green), MMLV (red), and water (blue). Arrows at the top indicate the positions of the **4W**, **3W**, and **2W** minima. Filled circles at the bottom indicate the umbrella points. The **4W**  $\rightarrow$  **3W** and **3W**  $\rightarrow$  **2W** barriers were computed as means of three trajectories with errors of  $\pm 0.3$  and  $\pm 0.8$  kcal/mol, respectively. The barriers computed using the Ewald summation and a nonbonding cutoff differed by  $<1.5$  kcal/mol (see the Supporting Information).

sampling<sup>11</sup> using the CHARMM34 program.<sup>12</sup> The reaction coordinate for binding of an outer-shell carboxylate to  $Mg^{2+}$  was chosen as the mean of the two  $Mg-O$  distances (Figure 2). To elucidate the role of the protein matrix, the corresponding barriers in pure water were also computed. Through a comparison of the free-energy profiles for the same reaction in different media (enzyme vs water), nonadditive effects in the force field would largely cancel.

Figure 3 shows that the qualitative effect of the protein matrix is to raise the free-energy barrier for binding of an outer-shell carboxylate to  $Mg^{2+}$ , although the quantitative effect depends on the enzyme. The barriers for the **4W**  $\rightarrow$  **2W** transition in RNase H from MMLV (21 kcal/mol), *E. coli* (18 kcal/mol), and HIV-1 (17 kcal/mol) are significantly greater than that in water (11 kcal/mol). The barrier for the **3W**  $\rightarrow$  **2W** transition in the two viral enzymes (7–8 kcal/mol) is also greater than that in water or in *E. coli* RNase HI ( $\sim 3$  kcal/mol).

The present results have two implications: (1) The protein matrix could play a role in catalysis by inducing a high barrier that may temporarily prevent conversion of **4W** to **2W**. This duration may suffice for the enzyme to catalyze the reaction, during which it could utilize the water-rich **4W** mode with a free outer-shell carboxylate to act as a proton or H-bond acceptor during catalysis. (2) Two drug candidates may possess similar free energies for binding to a given drug target protein, but one may encounter a larger kinetic barrier than the other upon protein binding. However, in current drug design, ligands are docked into the target pocket, and the drug candidate is selected on the basis of the free-energy difference between the bound and unbound states, excluding the free-energy barrier connecting the two states.

In conclusion, this study has demonstrated the role of the protein matrix in selecting a particular binding mode of its natural cofactor among other various energetically favorable binding modes. In the case of RNase H, the protein matrix raises the free-energy barrier for binding of a conserved, catalytically important outer-shell Asp to  $Mg^{2+}$ . Further studies are required for delineation of the geometric factors and/or interaction networks in RNase H that dictate the effects found herein.

**Acknowledgment.** This work was supported by the National Science Council through Research Grants NSC 93-2321-B-001-021 (to C.S.B.) and NSC 95-2113-M-001-001 (to C.L.) and by Academia Sinica.

**Supporting Information Available:** Details of the methodology. This material is available free of charge via the Internet at <http://pubs.acs.org>.

## References

- (1) Sigel, H. *Metal Ions in Biological Systems*; Marcel Dekker: New York, 1974. *Handbook on Metalloproteins*; Bertini, I., Sigel, A., Sigel, H., Eds.; Marcel Dekker: New York, 2001. Cowan, J. A. *Biological Chemistry of Magnesium*; VCH: New York, 1995.
- (2) Hostomsky, Z.; Hostomska, Z.; Matthews, D. A. In *Nucleases*, 2nd ed.; Linn, S. M., Lloyd, S., Roberts, R. J., Eds.; Cold Spring Harbor Monograph Series 25; Cold Spring Harbor Laboratory: Cold Spring Harbor, NY, 1994. Yang, W.; Steitz, T. A. *Structure* **1995**, *3*, 131. Venclovas, C.; Siksnys, V. *Nat. Struct. Biol.* **1995**, *2*, 838. Nicholson, A. W. In *Ribonucleases: Structures and Functions*; D'Alessio, G., Riordan, J. F., Eds.; Academic Press: New York, 1997.
- (3) Nowotny, M.; Gaidamakov, S. A.; Crouch, R. J.; Yang, W. *Cell* **2005**, *121*, 1005.
- (4) Lim, D.; Gregorio, G.; Bingman, C.; Martinez-Hackert, E.; Hendrickson, W. A.; Goff, S. P. *J. Virol.* **2006**, *80*, 8379.
- (5) Katayanagi, K.; Ishikawa, M.; Morikawa, K. *Proteins: Struct., Funct., Genet.* **1993**, *17*, 337. Kanaya, S.; Kohara, A.; Miura, Y.; Sekiguchi, A.; Iwai, S.; Inoue, H.; Ohtsuka, E.; Ikehara, M. *J. Biol. Chem.* **1990**, *265*, 4615.
- (6) Pari, K.; Mueller, G. A.; DeRose, E. F.; Kirby, T. W.; London, R. E. *Biochemistry* **2003**, *42*, 639.
- (7) Humphrey, W.; Dalke, A.; Schulten, K. *J. Mol. Graphics* **1996**, *14*, 33.
- (8) Casareno, R. L. B.; Li, D.; Cowan, J. A. *J. Am. Chem. Soc.* **1995**, *117*, 11011. Black, C. B.; Cowan, J. A. *Inorg. Chem.* **1994**, *33*, 5805.
- (9) Marcus, Y. *Chem. Rev.* **1988**, *88*, 1475.
- (10) Babu, C. S.; Dudev, T.; Casareno, R.; Cowan, J. A.; Lim, C. *J. Am. Chem. Soc.* **2003**, *125*, 9318.
- (11) Allen, M. P.; Tildesley, D. J. *Computer Simulation of Liquids*; Oxford University Press: New York, 1987. Kottalam, J.; Case, D. A. *J. Am. Chem. Soc.* **1988**, *110*, 7690.
- (12) Brooks, B. R.; Brucoleri, R. E.; Olafson, B. D.; States, D. J.; Swaminathan, S.; Karplus, M. *J. Comput. Chem.* **1983**, *4*, 187.

JA101494M